

# Fermionic quantum computation with Cooper pair splitters

Kostas Vilkelis<sup>1\*</sup>, <sup>2</sup>, Antonio Manesco<sup>2†</sup>, Juan Daniel Torres Luna<sup>1</sup>, Sebastian Miles<sup>1</sup>,  
Michael Wimmer<sup>1</sup>, Anton Akhmerov<sup>2</sup>

**1** Qutech, Delft University of Technology, Delft 2600 GA, The Netherlands

**2** Kavli Institute of Nanoscience, Delft University of Technology, Delft 2600 GA, The Netherlands

\* kostasvilkelis@gmail.com, †am@antoniomanesco.org

September 4, 2023

## Abstract

We propose a practical implementation of a universal quantum computer that uses local fermionic modes (LFM) rather than qubits. Our design consists of quantum dots tunnel coupled by a hybrid superconducting island together with a tunable capacitive coupling between the dots. We show that coherent control of Cooper pair splitting, elastic cotunneling, and Coulomb interactions allows us to implement the universal set of quantum gates defined by Bravyi and Kitaev [1]. Finally, we discuss possible limitations of the device and list necessary experimental efforts to overcome them.

---

## Contents

<b>1</b>	<b>Introduction</b>	<b>2</b>
<b>2</b>	<b>Design</b>	<b>2</b>
<b>3</b>	<b>Effective Hamiltonian</b>	<b>4</b>
3.1	Tunnel coupling	4
3.2	Capacitive coupling	5
<b>4</b>	<b>Fermionic quantum gates</b>	<b>6</b>
4.1	Unitary gate operations	6
4.2	Finite Zeeman splitting in the middle dot	7
4.3	Gate performance	7
<b>5</b>	<b>Future directions</b>	<b>8</b>
<b>6</b>	<b>Summary</b>	<b>9</b>
	<b>References</b>	<b>10</b>
<b>A</b>	<b>Schieffer-Wolff transformation</b>	<b>13</b>
<b>B</b>	<b>Convenience of the anti-parallel spin configuration</b>	<b>14</b>
B.1	Orthogonality with symmetric spin precession	14
B.2	Stability and number of operations	15

---

## 1 Introduction

Over the years, qubits emerged as the de facto basis for quantum computation with a plethora of host platforms: superconducting circuits [2,3], trapped ions [4,5] and quantum dots [6], to name a few. Recent works used qubit-based quantum computers to simulate fermionic systems [7–9]. However, the mapping from qubits to local fermionic modes (LFMs) is inefficient because it introduces additional overhead to the calculations [10, 11]. For example, a map from  $n$  qubits to fermions requires  $O(n)$  additional operations through the Jordan-Wigner transformation [12] and  $O(\log n)$  through the Bravyi-Kitaev transformation [1].

An alternative to avoid the overhead in the qubit to LFM map is to use a quantum computer that already operates with local fermionic modes [1]. Moreover, the advantage of local fermionic modes is not limited to the simulation of fermionic systems. A set of  $2n$  local fermionic modes maps directly to  $n$  parity-preserving qubits, which corresponds to  $n - 1$  qubits. Therefore, the map from local fermionic modes to qubits only requires a constant number of operations regardless of the system size and is, therefore, more efficient than the reverse [1]. Recently, Ref. [13, 14] showed that local fermionic modes offer advantages in quantum optimization problems of finding the ground state energy of fermionic Hamiltonians.

Motivated by this advantage of local fermionic modes over qubits, we propose an experimental implementation of a quantum computer with local fermionic modes. Our device is inspired by recently reported Cooper pair splitters [15–20], and our design includes an additional tunable capacitance to control Coulomb interactions. We show that the device implements the necessary universal set of gates proposed by Bravyi and Kitaev [1]. We also discuss the limitations of the device.

## 2 Design

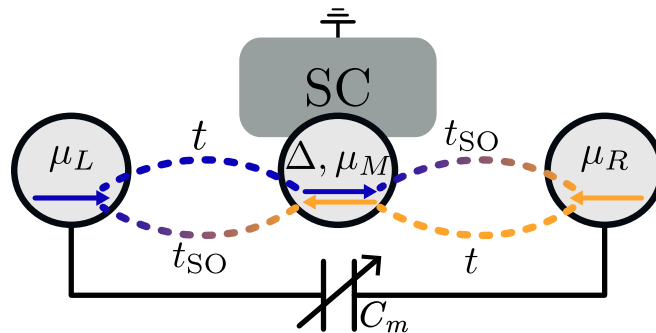


Figure 1: The unit cell of a fermionic quantum computer. Two singly-occupied spin-(anti)polarized quantum dots host the local fermionic modes  $L$  and  $R$ . Two tunnel barriers enable normal  $t$  and spin-dependent  $t_{SO}$  tunnelings between the two dots. A middle superconducting island mediates superconducting correlations between the two local fermionic modes. An external mutual capacitor  $C_m$  allows Coulomb interactions between the sites.

Bravyi and Kitaev [1] showed that fermionic quantum computation is equivalent to parity-preserving qubit operations. As a consequence, given a set of fermionic creation

$(c_i^\dagger)$  and annihilation operators  $(c_i)$ , it follows that

$$\left\{ \begin{array}{l} \mathcal{U}_1(\alpha) = \exp\left(i\alpha c_i^\dagger c_i\right), \quad \mathcal{U}_2(\beta) = \exp\left[i\beta\left(c_i^\dagger c_j + c_j^\dagger c_i\right)\right], \\ \mathcal{U}_3(\gamma) = \exp\left[i\gamma\left(c_i^\dagger c_j^\dagger + c_j c_i\right)\right], \quad \mathcal{U}_4(\delta) = \exp\left(i\delta c_i^\dagger c_i c_j^\dagger c_j\right) \end{array} \right\} \quad (1)$$

with  $\alpha = \beta = \gamma = \pi/4$ , and  $\delta = \pi$ , is a universal set of gate operators. The case of two LFMs is similar to two uncoupled qubits: each operation within a given fermion parity sector is a rotation within  $SU(2)$ . In the odd fermion parity sector, the operations  $\mathcal{U}_1(\alpha)$  and  $\mathcal{U}_2(\beta)$  are rotations around perpendicular axes in the Bloch sphere. Likewise  $\mathcal{U}_3(\gamma)$  and  $\mathcal{U}_4(\delta)$  are perpendicular rotations within the even fermion parity sector. In the presence of an extra ancilla LFM, applying  $\mathcal{U}_4$  entangles the even and odd subspaces of the two computational LFMs.

We thus propose a device where excitations occupy single-orbital sites, numbered by the subindex  $i$  and  $j$ . A practical platform for such a proposal is an array of spin-polarized quantum dots, as the scheme shown in Fig. 1. Within this platform, the unitary operations in Eq. 1 are a time-evolution of the following processes:

1.  $c_i^\dagger c_i$  onsite energy shift of the fermionic state at site  $i$ ;
2.  $c_i^\dagger c_j$  hopping of a fermion between sites  $i$  and  $j$ ;
3.  $c_i^\dagger c_j^\dagger$  superconducting pairing between fermions at sites  $i$  and  $j$ ;
4.  $c_i^\dagger c_i c_j^\dagger c_j$  Coulomb interaction between fermions at sites  $i$  and  $j$ .

We control the onsite energies  $\mu_i$  with plunger gates. Similarly, a tunnel gate between neighboring pairs of quantum dots controls hopping strength  $t$  between them. Manipulation with plunger and tunnel gates is a well-established technique in charge [21, 22] and spin [6] qubits.

To implement the superconducting coupling between the spin-polarized dots, we utilize the design of a triplet Copper pair splitter [16–20]. We include an auxiliary quantum dot in proximity to an s-wave superconductor mediating crossed Andreev reflection (CAR) and elastic cotunelling (ECT) between the two quantum dots that encode the LFMs. Thus, the ECT rate  $\Gamma$  sets the hopping strength between the two dots, whereas the CAR rate  $\Lambda$  sets the effective superconducting pairing. Because the dots are spin-polarised, the superconducting pairing must be of spin-triplet, enabled by spin-orbit hopping in the hosting material. We quantify the spin-orbit coupling in the hosting material by the spin precession angle between the dots  $\theta_i = 2\pi d/l_{so}$ , where  $d$  is the interdot distance and  $l_{so}$  is the spin-orbit length. The spin-orbit coupling in InSb wires leads to a spin-precession length  $l_{so} \approx 100$  nm [23, 24] resulting on non-negligible  $\theta_i$  within the order of dot-to-dot distance.

Finally, we achieve Coulomb interaction between a pair of dots through capacitive coupling  $C_m$ . Our design requires a variable capacitive coupling to implement the  $\mathcal{U}_4$  gate. Several recent works demonstrate variable capacitive coupling in various platforms: gate-tunable two-dimensional electron gas [25], varactor diodes [26], and external double quantum dots [27].

We show the unit cell of a fermionic quantum computer with two LFMs in Fig. 1. The basic building block consists of three tunnel-coupled quantum dots in a material with large spin-orbit coupling. The middle dot is proximitized by an s-wave superconductor with an induced gap  $\Delta$  that mediates CAR and ECT between the outer dots. The spin-polarised outer dots ( $L, R$ ) encode the LFMs, whereas the middle one is an auxiliary component.

Finally, a tunable capacitor couples the outer dots. We generalize the device to an arbitrary number of LFMs by repeating the unit cell in a chain. To read out the fermionic state, we propose to measure the occupation in each quantum dot through charge sensing [28].

### 3 Effective Hamiltonian

#### 3.1 Tunnel coupling

In the absence of capacitive and tunnel coupling, the approximate Hamiltonian for the two spin-polarised dots is

$$H_d = \sum_{i=L,R} \mu_i c_{i\sigma}^\dagger c_{i\sigma} , \quad (2)$$

where  $c_{i\sigma}$  is the electron annihilation operator at site  $i$  and spin  $\sigma$ , and  $\mu_i$  is the corresponding chemical potential. The Hamiltonian in Eq. (2) is valid if the charging energy and Zeeman splitting on each dot are larger than all other energy scales in the problem. Recent experiments on similar devices measure charging energy of 2 meV and Zeeman splitting of 400  $\mu$ eV at 200 mT [16, 17, 19, 20]. Both charging energy and Zeeman splitting are larger than the usual induced superconducting gap inside the quantum dot  $\Delta \sim 100 \mu$ eV [20, 29, 30], justifying the approximation in Eq. (2).

The proximity of the middle dot to the superconductor suppresses its  $g$ -factor [31]. Thus, differently from the outer dots, we consider a finite Zeeman energy  $B$ . The Hamiltonian of the middle dot is

$$H_{\text{ABS}} = \sum_{\sigma,\sigma'} [\mu_M(\sigma_0)_{\sigma\sigma'} + B(\sigma_z)_{\sigma\sigma'}] c_{M\sigma}^\dagger c_{M\sigma'} + \Delta c_{M\uparrow}^\dagger c_{M\downarrow}^\dagger + \text{h.c.} \quad (3)$$

where  $c_{M\sigma}^\dagger$  is the creation operator of electron on the middle dot with spin  $\sigma$ ,  $\Delta$  is the induced superconducting gap, and  $\sigma_l$  are the Pauli matrices ( $l = \{0, x, y, z\}$ ) acting on the spin subspace. Both spin-polarised dots in Eq. (2) connect to the middle dot by symmetric tunnel barriers with strength  $t$ . The barrier  $t$  controls both normal and spin-orbit tunneling processes:

$$H_t = t \sum_{i=L,R} \cos \theta_i c_{i\sigma}^\dagger c_{M\sigma} + it \sum_{i=L,R} \sum_{\sigma'} (\sigma_y)_{\sigma_i\sigma'} \sin \theta_i c_{i\sigma}^\dagger c_{M\sigma'} + \text{h.c.} , \quad (4)$$

where  $\theta_i$  is the spin precession angle from dot  $i$  to the middle island. Thus, the total Hamiltonian is

$$H = H_d + H_{\text{ABS}} + H_t . \quad (5)$$

We obtain the effective low-energy Hamiltonian in the weak-coupling limit,  $t \ll \Delta$ , through a Schrieffer-Wolf (the derivation is in Appendix A) [32, 33]:

$$\tilde{H} = \sum_i \epsilon_i^{\sigma_i\sigma_j} c_{i\sigma_i}^\dagger c_{i\sigma_i} + \sum_{i,j} \Gamma_{\sigma_i\sigma_j} c_{i\sigma_i}^\dagger c_{j\sigma_j} + \Lambda_{\sigma_i\sigma_j} c_{i\sigma_i}^\dagger c_{j\sigma_j}^\dagger + \text{h.c.} , \quad (6)$$

where  $\epsilon_i^{\sigma_i\sigma_j}$  is the renormalised onsite energy of dot  $i$ ,  $\Gamma_{\sigma_i\sigma_j}$  is the ECT rate and  $\Lambda_{\sigma_i\sigma_j}$  is the CAR rate. While  $t \neq 0$ , we do not vary the chemical potential of the outer dots,  $\mu_L = \mu_R = 0$ . For simplicity, we also assume no Zeeman splitting within the middle dot  $B = 0$  and that the spin precession angles are symmetric  $\theta_L = \theta_R = \theta$  (see Appendix A for more general form). In such case, the effective parameters for the anti-parallel spin configuration are:

$$\Lambda_{\uparrow\downarrow} = \kappa \Delta \cos(2\theta) , \quad \Gamma_{\uparrow\downarrow} = -i\kappa \mu_M \sin(2\theta) , \quad (7)$$

and for the parallel channel:

$$\Lambda_{\uparrow\uparrow} = -i\kappa\Delta \sin(2\theta), \quad \Gamma_{\uparrow\uparrow} = -\kappa\mu_M \cos(2\theta), \quad (8)$$

where

$$\kappa = t^2/(\Delta^2 + \mu_M^2 - B^2). \quad (9)$$

Both onsite corrections terms are equal:

$$\epsilon_L^{\sigma_i\sigma_j} = \epsilon_R^{\sigma_i\sigma_j} = \kappa\mu_M. \quad (10)$$

We observe that the magnitude of  $\Lambda_{\sigma_i\sigma_j}$  is maximum at  $\mu_M = 0$  and drops with increasing chemical potential  $\mu_M$ . On the other hand,  $\Gamma_{\sigma_i\sigma_j}$  has maxima at finite  $\mu_M$ . The magnitude of both processes depends on the spin-precession angle  $\theta$  and spin configuration of the outer dots as shown in Fig. 2 (a) and (b). To ensure that operation times for  $\mathcal{U}_2$  and  $\mathcal{U}_3$  are similar, the convenient regime is where  $\max \Gamma_{\sigma_i\sigma_j} \sim \max \Lambda_{\sigma_i\sigma_j}$ .

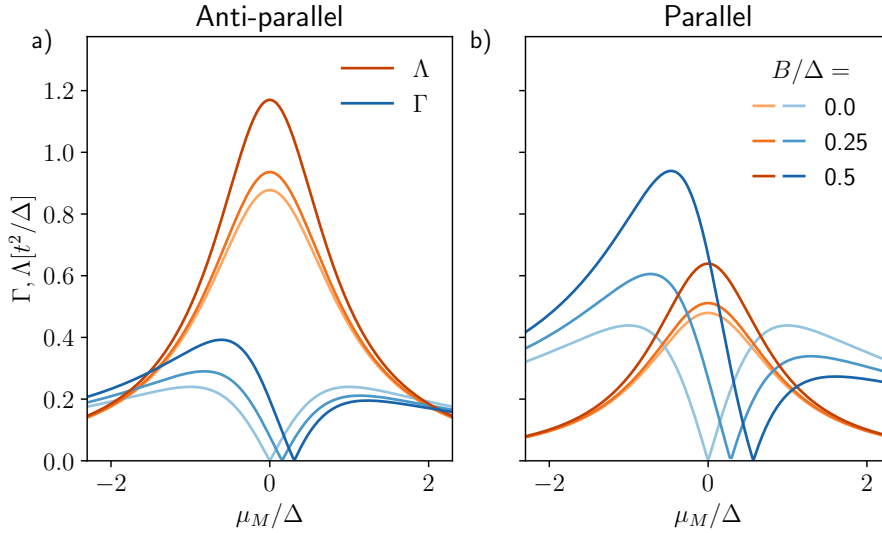


Figure 2: Absolute value of  $\Lambda$  (blue) and  $\Gamma$  (orange) as a function of  $\mu_M$  for different values of  $B$  for the anti-parallel configuration (a) and the parallel configuration (b). System parameters are  $t = 0.15$ ,  $\theta_L = 0.7$  and  $\theta_R = 0.3$ .

### 3.2 Capacitive coupling

The electrostatic energy between the two dots is [34]:

$$H_C = \sum_{i=L,R} v_i c_{i\sigma_i}^\dagger c_{i\sigma_i} + U_m c_{L\sigma_L}^\dagger c_{L\sigma_L} c_{R\sigma_R}^\dagger c_{R\sigma_R}, \quad (11)$$

where  $U_m = C_m e^2 / \tilde{C}$  is the mutual interaction between the two dots,

$$v_{L/R} = \frac{C_{R/L}(2n_{g,L/R} + 1) + C_m n_{g,R/L}}{2\tilde{C}} \quad (12)$$

is the renormalization to the onsite energy,  $\tilde{C} = C_L C_R - C_m^2$ ,  $C_L$  and  $C_R$  are the capacitances of the left and right dots,  $C_m$  is the mutual capacitance, and  $n_{g,i}$  is the charge offset in the site  $i$ . Notice that we consider singly-occupied dots in (11). This approximation is valid when  $U_m \ll \Delta \ll e^2 C_{L/R} / \tilde{C}$  because the charging energy renormalization due to the mutual capacitance is negligible in this regime. The last term in (11) gives the Coulomb interaction between the dots required to implement  $\mathcal{U}_4$ .

## 4 Fermionic quantum gates

### 4.1 Unitary gate operations

To achieve the fermionic quantum operations defined in Eq. (1), we need to engineer specific time-dependent profiles for the tunable system parameters. In this case, we control the following system parameters through Eqs. (11) and (6): left and right plunger gates ( $\mu_L, \mu_R$ ), middle plunger gate ( $\mu_M$ ), tunnel gates ( $t$ , we treat the two tunnel gates together), and mutual capacitance ( $C_m$ ). For simplicity, we only consider square pulses in time

$$H(\tau) = H_P(S)[\Theta(\tau) - \Theta(\tau - \tau_P)] \quad (13)$$

where  $\Theta(\tau)$  is the Heaviside step function,  $\tau$  is time and  $\tau_P$  is the duration of the pulse. We define the pulse Hamiltonian  $H_P(S)$  as a constant total Hamiltonian where  $S = \{t, \mu_M, \dots\}$  are non-zero system parameters in the pulse. For example,  $H_P(\{t\})$  is a constant Hamiltonian with all system parameters zero except the tunnel coupling  $t$ . We set the idle (reference) Hamiltonian to one where all gates are zero,  $t = \mu_L = \mu_R = \mu_M = U = 0$ . Thus, the time-evolution operator simplifies to

$$\mathcal{U}(\tau_2, \tau_1) = \exp \left[ -\frac{i}{\hbar} \int_{\tau_1}^{\tau_2} d\tau' H(\tau') \right] = \exp \left[ -\frac{i}{\hbar} H_P(S) \tau_P \right]. \quad (14)$$

where  $\tau_2, \tau_1$  are the initial and final times, and  $\tau_P$  is the duration of the pulse. In practice, the transition between the idle Hamiltonian and  $H_P$  in Eq. (13) is not instantaneous but ramps up smoothly over a time  $\tau_R$  to minimize non-adiabatic transitions.

We engineer the unitary operations as an ordered sequence of pulses defined in Eq. (14). For simplicity, we assume no Zeeman splitting in the middle dot,  $B = 0$ , and leave the discussion of the more general case to section 4.2. In this case, the minimal pulse sequence scheme which implements the gates in Eq. (1) is:

1. onsite operation:

$$\mathcal{U}_1 = \exp \left[ -\frac{i}{\hbar} H_P(\{\mu_L, \mu_R\}) \tau_P \right]; \quad (15)$$

2. hopping operation:

$$\begin{aligned} \mathcal{U}_2 = & \exp \left[ -\frac{i}{\hbar} H_P(\{\mu_L = \mu, \mu_R = \mu\}) \tau_P^{(4)} \right] \times \exp \left[ -\frac{i}{\hbar} H_P(\{t\}) \tau_P^{(3)} \right] \\ & \times \exp \left[ -\frac{i}{\hbar} H_P(\{\mu_L = \mu, \mu_R = \mu\}) \tau_P^{(2)} \right] \times \exp \left[ -\frac{i}{\hbar} H_P(\{t, \mu_M\}) \tau_P^{(1)} \right] \end{aligned} \quad (16)$$

3. superconducting pairing operation:

$$\mathcal{U}_3 = \exp \left[ -\frac{i}{\hbar} H_P(\{t\}) \tau_P \right]; \quad (17)$$

4. Coulomb interaction operation:

$$\mathcal{U}_4 = \exp \left[ -\frac{i}{\hbar} H_P(\{\mu_L, \mu_R\}) \tau_P^{(2)} \right] \times \exp \left[ -\frac{i}{\hbar} H_P(\{U\}) \tau_P^{(1)} \right]; \quad (18)$$

where we indicate as  $\tau_P^{(i)}$  the duration of the  $i$ -th pulse.

In the above scheme, the operations  $\mathcal{U}_1$  and  $\mathcal{U}_3$  require a single pulse. The gate  $\mathcal{U}_1$  requires a single pulse because the dots are uncoupled from one another and the plunger gates affect the onsite energies without inducing any sort of coupling between the dots. Similarly,  $\mathcal{U}_3$  is also a single operation because the CAR rate is maximum at  $\mu_M = 0$  whereas both ECT rate and onsite corrections are zero according to Eqs. (7–10). We show the time-dependent simulation of the  $\mathcal{U}_3$  gate in Fig. 3.

On the other hand, the first pulse of Eq. (16) introduces finite onsite corrections to the outer dots and CAR according to Eqs. (7–10). Since the onsite corrections are equal, only a global phase factor is accumulated within the odd fermion parity sector. On the other hand, both onsite corrections and CAR result in undesired rotations within the even fermion parity subspace. We undo these operations with an Euler rotation using two orthogonal operations, resulting in the three subsequent pulses in Eq. (16). Similarly, the Coulomb operation in Eq. (18) also requires a correction pulse with the plunger gates because the mutual capacitance  $C_m$  renormalizes the onsite energies in the outer dots, as shown in Eq. (11).

## 4.2 Finite Zeeman splitting in the middle dot

The presence of Zeeman splitting in the middle dot  $B$  introduces (see Appendix A) an asymmetric onsite renormalisation  $\epsilon_L^{\sigma_i\sigma_j} \neq \epsilon_R^{\sigma_i\sigma_j}$  and a shift in the minima of  $\Gamma_{\sigma_i\sigma_j}$  shifts away from  $\mu_M = 0$ , as shown in Fig. 2. These changes affect the prescriptions for  $\mathcal{U}_2$  and  $\mathcal{U}_3$  since these operations require finite  $t$ .

The asymmetric onsite corrections break the orthogonality between  $\mathcal{U}_1$  and the unitary operation prescribed in Eq. (16). It is still possible to implement the  $\mathcal{U}_2$  with two non-orthogonal rotation axes in the odd fermion parity sector with additional operations to compensate for the non-orthogonality [35].

The operation in Eq. (17) also introduces finite  $\Gamma_{\sigma_i\sigma_j}$  in the odd parity sector. We show in Appendix B that anti-parallel spin configuration with symmetric spin-orbit precession  $\theta_L = \theta_R$  removes the shifting  $\Lambda$  minima away from  $\mu_M = 0$  and restores the orthogonality of the operations within the even parity sector.

## 4.3 Gate performance

Switching on the pulse in Eq. (13) happens over a finite rise time  $\tau_R$ . Short rise times  $\tau_R$  induce transitions from the LFM dots into the middle ABS at energy  $\sim \Delta$  which limits the performance of the gates. To avoid such transitions, the pulse times need to be  $\tau_R \gg \hbar/\Delta$ . In Fig. 2 we show the time-dependent simulation of the gate  $\mathcal{U}_3$  with different rise times. We find that rise times  $\tau_R > 2\hbar/\Delta$  ensures negligible transitions into the ABS. In a system of  $\Delta = 100 \mu\text{eV}$  that corresponds to rise times of  $\tau_R > 13 \text{ ps}$ .

Current tunable capacitors [25, 26] vary over a limited range. The upper limit for the ratio between the maximum and minimum capacitance  $r = C_{\text{off}}/C_{\text{on}}$  is  $r \approx 40$  [25, 26]. Thus, there is a non-negligible residual capacitance between the dots when the  $\mathcal{U}_4$  gate is off. This residual capacitance acts as an unwanted source of phase and limits the performance of the device. Because such error is coherent, we argue it is possible to offset it after each or a few operations with a compensating  $\mathcal{U}_4$  pulse. However, since  $[\mathcal{U}_3, \mathcal{U}_4] \neq 0$ , the  $\mathcal{U}_3$  operation would require similar compensation pulses to Eq. (16) to offset the effect of the residual capacitor.

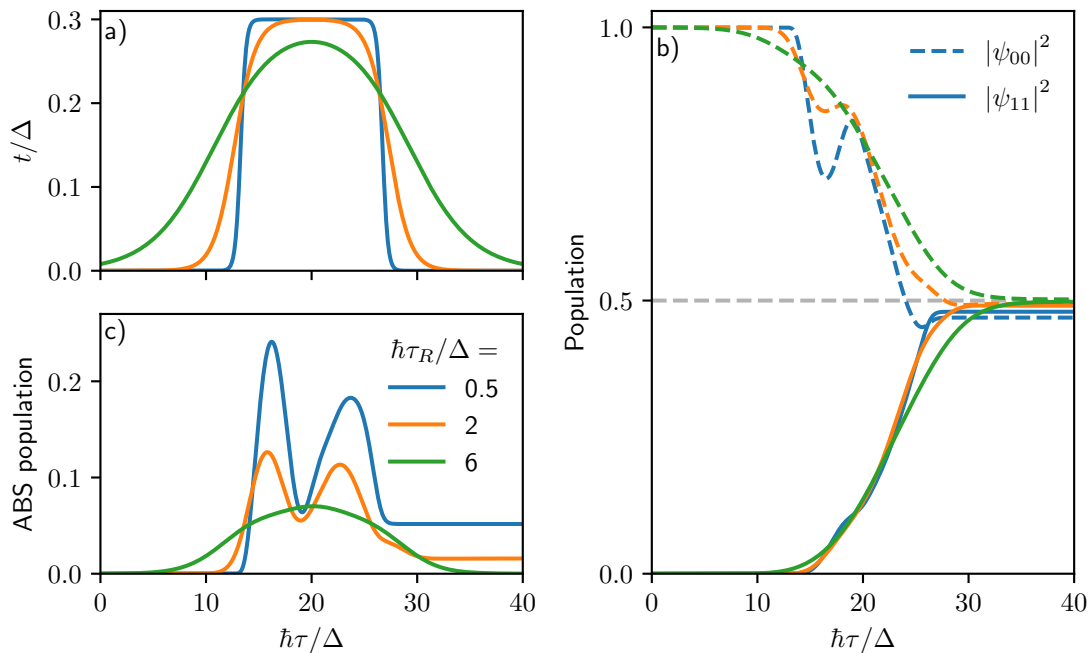


Figure 3: Time-dependent simulation of pairing gate  $\mathcal{U}_3$  acting on an initial vacuum state with different pulse rise time  $\tau_R$  profiles. The vacuum population is  $|\psi_{00}\rangle^2$  whereas the double occupation population (with middle dot unoccupied) is  $|\psi_{11}\rangle^2$ . Longer pulses (a) result in a smoother transient population profile (b) and less leakage into the middle ABS state (c). The configuration is the spin-antiparallel with finite Zeeman field within the middle dot  $B/\Delta = 0.2$  and symmetric spin-orbit precession  $\theta_L = \theta_R = \pi/8$

## 5 Future directions

Although the device we proposed has the ingredients to implement universal fermionic gates, further work is required to mitigate the main sources of errors. Because of its similarities to a quantum dot charge qubit, we expect the limiting decoherence mechanism to be the same - charge noise [36]. Typical coherence times are on the order of a few nanoseconds [21, 36–38]. In comparison, Dvir et al. [20] reports CAR/ECT strengths of  $\hbar/\Gamma_{\text{CAR/ECT}} \approx 10 \mu\text{s}$  from which we estimate the gate pulse of our proposed device to be  $\approx 50 \text{ ps}$ . On the other hand, if the outer dots in the device shown in Fig. 1 are also proximitized by a superconductor, the local fermionic modes would be encoded by Andreev quasiparticles. Because Andreev states are linear combinations of electron and hole-like excitations, it is possible to design a device that operates with neutral fermions. A similar idea was recently proposed to avoid charge noise in fermion-parity qubits [39]. Finally, minimization of the main sources of errors allows implementation of error-correction codes for fermionic systems [40].

In the current device, superconducting pairing persists under all possible parameters. Because of that, the hopping operation in Eq. (16) requires a complicated procedure in order to remove the effects of the induced superconducting gap. To simplify the hopping operation, we suggest using a device that allows control of the amount of induced superconducting pairing into the middle dot. For example, a tunnel barrier between the middle dot and the superconducting lead would mediate the induced superconducting pairing. Alternatively, connecting the middle dot to two superconducting leads and controlling the



phase difference between them would also allow to control the induced superconducting pairing.

Our proposed device consists of a chain of single-orbital fermionic sites. The device layout is a limiting factor, as it only allows nearest-neighbor hoppings, superconducting pairing, and electrostatic interactions. The layout limitations are detrimental to effective scalability. Thus, future works could for example generalize the model to, for example, two-dimensional lattices.

We showed that the proposed device is a building block of a fermionic quantum computer. However, we must also emphasize that the high control of the system parameters allows to use the same device as a quantum simulator. For example, a chain-like device with the unit cell shown in Fig. 1 at finite  $\Gamma$  and  $U$  can be directly mapped to the Heisenberg model. Thus, together with superconducting correlations, these devices would be an extension of other quantum dot platforms [41].

We mentioned in Sec. 4 that all tunable capacitors proposed present a residual mutual capacitance  $C_{\text{off}}$ . The external capacitor is necessary because direct mutual capacitance is suppressed by the charge screening in the superconducting island. On the other hand, a floating superconducting island offers a direct interdot capacitance [42]. In a device with a switch between a floating and grounded superconductor, there would be direct control of the mutual capacitance. Moreover, the large charge screening due to the grounded superconducting island sets  $C_{\text{off}} \approx 0$ , removing the need to fix offset phases due to the residual capacitance.

## 6 Summary

We showed that Copper pair-splitting devices with tunable capacitors make up a building block of a fermionic quantum computer. We derived the low-energy Hamiltonian and showed that it contains all the necessary processes to build a universal set of gate operations. Moreover, we showed how to use experimentally controllable parameters to implement the gate operations. We find that the presence of Zeeman splitting in the superconducting island complicates the implementation of gates and necessitates additional steps. Based on the low-energy theory, we also studied optimal regimes for the device operation. While our design was mostly inspired by recent experiments, we also discussed how to avoid foreseeable limitations such as (i) the use of neutral fermions to suppress charge noise; (ii) a floating superconducting island to simplify the layout; (iii) control of the superconducting gap to simplify gate operations.

## Acknowledgements

The authors acknowledge the inputs of: Isidora Araya Day on perturbation theory calculations; Mert Bozkurt and Chun-Xiao Liu on the device conception and development of an effective model; Christian Prosko, Valla Fatemi, David van Driel, Francesco Zatelli, and Greg Mazur on the experimental feasibility.

## Data Availability

All code used in the manuscript is available on Zenodo [32].

## Author contributions

A.A and M.W. formulated the initial project idea and advised on various technical aspects. K.V. and A.M. supervised the project. K.V., A.M. and J.T. developed the effective model and the device design. K.V., A.M., J.T, and S.M. constructed the gate operations. K.V. performed the time-dependent calculations. All authors contributed to the final version of the manuscript.

## Funding information

The project received funding from the European Research Council (ERC) under the European Union's Horizon 2020 research and innovation program grant agreement No. 828948 (AndQC). The work acknowledges NWO HOT-NANO grant (OCENW.GROOT.2019.004) and VIDI Grant (016.Vidi.189.180) for the research funding.

## References

- [1] S. B. Bravyi and A. Y. Kitaev, *Fermionic quantum computation*, Ann. Phys-new. York. **298**(1), 210 (2002), doi:10.1006/aphy.2002.6254.
- [2] M. H. Devoret and R. J. Schoelkopf, *Superconducting circuits for quantum information: An outlook*, Science **339**(6124), 1169 (2013), doi:10.1126/science.1231930.
- [3] M. Kjaergaard, M. E. Schwartz, J. Braumüller, P. Krantz, J. I.-J. Wang, S. Gustavsson and W. D. Oliver, *Superconducting qubits: Current state of play*, Annual Review of Condensed Matter Physics **11**(1), 369 (2020), doi:10.1146/annurev-conmatphys-031119-050605.
- [4] C. D. Bruzewicz, J. Chiaverini, R. McConnell and J. M. Sage, *Trapped-ion quantum computing: Progress and challenges*, Applied Physics Reviews **6**(2), 021314 (2019), doi:10.1063/1.5088164.
- [5] H. Häffner, C. Roos and R. Blatt, *Quantum computing with trapped ions*, Physics Reports **469**(4), 155 (2008), doi:https://doi.org/10.1016/j.physrep.2008.09.003.
- [6] G. Burkard, T. D. Ladd, A. Pan, J. M. Nichol and J. R. Petta, *Semiconductor spin qubits*, Rev. Mod. Phys. **95**, 025003 (2023), doi:10.1103/RevModPhys.95.025003.
- [7] A. Rahmani, K. J. Sung, H. Putterman, P. Roushan, P. Ghaemi and Z. Jiang, *Creating and manipulating a Laughlin-type  $\nu = 1/3$  fractional quantum hall state on a quantum computer with linear depth circuits*, PRX Quantum **1**(2) (2020), doi:10.1103/prxquantum.1.020309.
- [8] F. Arute, K. Arya, R. Babbush, D. Bacon, J. C. Bardin, R. Barends, A. Bengtsson, S. Boixo, M. Broughton, B. B. Buckley, D. A. Buell, B. Burkett *et al.*, *Observation of separated dynamics of charge and spin in the fermi-hubbard model* (2020), 2010.07965.
- [9] G. A. Quantum, Collaborators\*†, F. Arute, K. Arya, R. Babbush, D. Bacon, J. C. Bardin, R. Barends, S. Boixo, M. Broughton, B. B. Buckley, D. A. Buell *et al.*, *Hartree-fock on a superconducting qubit quantum computer*, Science **369**(6507), 1084 (2020), doi:10.1126/science.abb9811.

- [10] S. McArdle, S. Endo, A. Aspuru-Guzik, S. C. Benjamin and X. Yuan, *Quantum computational chemistry*, Rev. Mod. Phys. **92**, 015003 (2020), doi:10.1103/RevModPhys.92.015003.
- [11] J. D. Whitfield, J. Biamonte and A. Aspuru-Guzik, *Simulation of electronic structure hamiltonians using quantum computers*, Mol. Phys. **109**(5), 735 (2011), doi:10.1080/00268976.2011.552441.
- [12] A. S. Wightman, ed., *The Collected Works of Eugene Paul Wigner*, Springer Berlin Heidelberg, doi:10.1007/978-3-662-02781-3 (1993).
- [13] Y. Herasymenko, M. Stroeks, J. Helsen and B. Terhal, *Optimizing sparse fermionic hamiltonians*, Quantum **7**, 1081 (2023), doi:10.22331/q-2023-08-10-1081.
- [14] M. B. Hastings and R. O'Donnell, *Optimizing strongly interacting fermionic hamiltonians*, In *Proceedings of the 54th Annual ACM SIGACT Symposium on Theory of Computing*. ACM, doi:10.1145/3519935.3519960 (2022).
- [15] M. Leijnse and K. Flensberg, *Parity qubits and poor man's majorana bound states in double quantum dots*, Phys. Rev. B **86**(13) (2012), doi:10.1103/physrevb.86.134528.
- [16] Q. Wang, S. L. D. ten Haaf, I. Kulesh, D. Xiao, C. Thomas, M. J. Manfra and S. Goswami, *Triplet cooper pair splitting in a two-dimensional electron gas* (2022), 2211.05763.
- [17] G. Wang, T. Dvir, G. P. Mazur, C.-X. Liu, N. van Loo, S. L. D. ten Haaf, A. Bordin, S. Gazibegovic, G. Badawy, E. P. A. M. Bakkers, M. Wimmer and L. P. Kouwenhoven, *Singlet and triplet cooper pair splitting in hybrid superconducting nanowires*, Nature **612**(7940), 448 (2022), doi:10.1038/s41586-022-05352-2.
- [18] C.-X. Liu, G. Wang, T. Dvir and M. Wimmer, *Tunable superconducting coupling of quantum dots via andreev bound states in semiconductor-superconductor nanowires*, Phys. Rev. Lett. **129**, 267701 (2022), doi:10.1103/PhysRevLett.129.267701.
- [19] A. Bordin, G. Wang, C.-X. Liu, S. L. D. ten Haaf, G. P. Mazur, N. van Loo, D. Xu, D. van Driel, F. Zatelli, S. Gazibegovic, G. Badawy, E. P. A. M. Bakkers *et al.*, *Controlled crossed andreev reflection and elastic co-tunneling mediated by andreev bound states* (2022), 2212.02274.
- [20] T. Dvir, G. Wang, N. van Loo, C.-X. Liu, G. P. Mazur, A. Bordin, S. L. D. ten Haaf, J.-Y. Wang, D. van Driel, F. Zatelli, X. Li, F. K. Malinowski *et al.*, *Realization of a minimal kitaev chain in coupled quantum dots*, Nature **614**(7948), 445 (2023), doi:10.1038/s41586-022-05585-1.
- [21] D. Kim, D. R. Ward, C. B. Simmons, J. K. Gamble, R. Blume-Kohout, E. Nielsen, D. E. Savage, M. G. Lagally, M. Friesen, S. N. Coppersmith and M. A. Eriksson, *Microwave-driven coherent operation of a semiconductor quantum dot charge qubit*, Nature Nanotechnology **10**(3), 243 (2015), doi:10.1038/nnano.2014.336.
- [22] J. Gorman, D. G. Hasko and D. A. Williams, *Charge-qubit operation of an isolated double quantum dot*, Phys. Rev. Lett. **95**, 090502 (2005), doi:10.1103/PhysRevLett.95.090502.

- [23] M. W. A. de Moor, J. D. S. Bommer, D. Xu, G. W. Winkler, A. E. Antipov, A. Bargerbos, G. Wang, N. van Loo, R. L. M. O. het Veld, S. Gazibegovic, D. Car, J. A. Logan *et al.*, *Electric field tunable superconductor-semiconductor coupling in majorana nanowires*, *New J. Phys.* **20**(10), 103049 (2018), doi:10.1088/1367-2630/aae61d.
- [24] I. van Weperen, B. Tarasinski, D. Eeltink, V. S. Pribiag, S. R. Plissard, E. P. A. M. Bakkers, L. P. Kouwenhoven and M. Wimmer, *Spin-orbit interaction in insb nanowires*, *Phys. Rev. B* **91**, 201413 (2015), doi:10.1103/PhysRevB.91.201413.
- [25] N. Materise, M. C. Dartiailh, W. M. Strickland, J. Shabani and E. Kapit, *Tunable capacitor for superconducting qubits using an InAs/InGaAs heterostructure*, *Quantum Science and Technology* **8**(4), 045014 (2023), doi:10.1088/2058-9565/aceb18.
- [26] R. S. Eggli, S. Svab, T. Patlatiuk, D. Trüssel, M. J. Carballido, P. C. Kwon, S. Geyer, A. Li, E. P. A. M. Bakkers, A. V. Kuhlmann and D. M. Zumbühl, *Cryogenic hyperabrupt strontium titanate varactors for sensitive reflectometry of quantum dots* (2023), 2303.02933.
- [27] A. Hamo, A. Benyamini, I. Shapir, I. Khivrich, J. Waissman, K. Kaasbjerg, Y. Oreg, F. von Oppen and S. Ilani, *Electron attraction mediated by coulomb repulsion*, *Nature* **535**(7612), 395 (2016), doi:10.1038/nature18639.
- [28] W. Lu, Z. Ji, L. Pfeiffer, K. W. West and A. J. Rimberg, *Real-time detection of electron tunnelling in a quantum dot*, *Nature* **423**(6938), 422 (2003), doi:10.1038/nature01642.
- [29] S. T. Gill, J. Damasco, D. Car, E. P. A. M. Bakkers and N. Mason, *Hybrid superconductor-quantum point contact devices using InSb nanowires*, *Applied Physics Letters* **109**(23) (2016), doi:10.1063/1.4971394.
- [30] Önder Gül, H. Zhang, F. K. de Vries, J. van Veen, K. Zuo, V. Mourik, S. Conesa-Boj, M. P. Nowak, D. J. van Woerkom, M. Quintero-Pérez, M. C. Cassidy, A. Geresdi *et al.*, *Hard superconducting gap in InSb nanowires*, *Nano Letters* **17**(4), 2690 (2017), doi:10.1021/acs.nanolett.7b00540.
- [31] T. D. Stanescu and S. Das Sarma, *Proximity-induced low-energy renormalization in hybrid semiconductor-superconductor majorana structures*, *Phys. Rev. B* **96**, 014510 (2017), doi:10.1103/PhysRevB.96.014510.
- [32] K. Vilkelis, A. Manesco, J. D. Torres Luna, S. Miles, M. Wimmer and A. Akhmerov, *Fermionic quantum computation with Cooper pair splitters*, doi:10.5281/zenodo.8279302 (2023).
- [33] I. Araya Day, S. Miles, D. Varjas and A. R. Akhmerov, *Pymablock*, doi:10.5281/zenodo.7995684 (2023).
- [34] W. G. van der Wiel, S. De Franceschi, J. M. Elzerman, T. Fujisawa, S. Tarucha and L. P. Kouwenhoven, *Electron transport through double quantum dots*, *Rev. Mod. Phys.* **75**, 1 (2002), doi:10.1103/RevModPhys.75.1.
- [35] M. Hamada, *The minimum number of rotations about two axes for constructing an arbitrarily fixed rotation*, *Royal Society Open Science* **1**(3), 140145 (2014), doi:10.1098/rsos.140145.

- [36] K. D. Petersson, J. R. Petta, H. Lu and A. C. Gossard, *Quantum coherence in a one-electron semiconductor charge qubit*, Phys. Rev. Lett. **105**, 246804 (2010), doi:10.1103/PhysRevLett.105.246804.
- [37] B. P. Wuetz, D. D. Esposti, A.-M. J. Zwerver, S. V. Amitonov, M. Botifoll, J. Arbiol, A. Sammak, L. M. K. Vandersypen, M. Russ and G. Scappucci, *Reducing charge noise in quantum dots by using thin silicon quantum wells*, Nature Communications **14**(1) (2023), doi:10.1038/s41467-023-36951-w.
- [38] J. W. G. van den Berg, S. Nadj-Perge, V. S. Pribiag, S. R. Plissard, E. P. A. M. Bakkers, S. M. Frolov and L. P. Kouwenhoven, *Fast spin-orbit qubit in an indium antimonide nanowire*, Phys. Rev. Lett. **110**, 066806 (2013), doi:10.1103/PhysRevLett.110.066806.
- [39] M. Geier, R. S. Souto, J. Schulenburg, S. Asaad, M. Leijnse and K. Flensberg, *A fermion-parity qubit in a proximitized double quantum dot* (2023), 2307.05678.
- [40] S. Vijay and L. Fu, *Quantum error correction for complex and majorana fermion qubits* (2017), 1703.00459.
- [41] C. van Diepen, T.-K. Hsiao, U. Mukhopadhyay, C. Reichl, W. Wegscheider and L. Vandersypen, *Quantum simulation of antiferromagnetic heisenberg chain with gate-defined quantum dots*, Physical Review X **11**(4) (2021), doi:10.1103/physrevx.11.041025.
- [42] F. K. Malinowski, R. K. Rupesh, L. Pavešić, Z. Guba, D. de Jong, L. Han, C. G. Prosko, M. Chan, Y. Liu, P. Krogstrup, A. Pályi, R. Žitko *et al.*, *Quantum capacitance of a superconducting subgap state in an electrostatically floating dot-island* (2022), 2210.01519.

## A Schieffer-Wolff transformation

To obtain the effective Hamiltonian from Eq. (6), we perform a Schieffer-Wolff transformation. We, first, diagonalize the Hamiltonian of the middle dot in Eq. (3):

$$H_{\text{ABS}} = (\epsilon_{\text{ABS}} + B)\gamma_{\uparrow}^{\dagger}\gamma_{\uparrow} + (\epsilon_{\text{ABS}} - B)\gamma_{\downarrow}^{\dagger}\gamma_{\downarrow}, \quad (19)$$

where  $\epsilon_{\text{ABS}} = \sqrt{\Delta^2 + \mu_M^2}$ ,  $\gamma_{\sigma}$  are the annihilation operators of Andreev quasiparticles

$$\gamma_{\uparrow}^{\dagger} = uc_{M\uparrow}^{\dagger} + vc_{M\downarrow}, \quad \gamma_{\downarrow}^{\dagger} = uc_{M\downarrow}^{\dagger} - vc_{M\uparrow}, \quad (20)$$

and  $u$  and  $v$  are the coherence factors.

We now define the occupation basis for the many-body states as  $|n_L, n_M, n_R\rangle$ , where  $n_i$  corresponds to the occupation number at the site  $i$ . Notice that for the middle dot, we define the number operator as  $\hat{n}_{M\sigma} = \gamma_{M\sigma}^{\dagger}\gamma_{M\sigma}$ , whereas in the outer dots  $\hat{n}_{i\sigma_i} = c_{i\sigma_i}^{\dagger}c_{i\sigma_i}$ . Because we consider  $\mu_{L/R}, B \ll \Delta$ , in the absence of hopping between the dots,

$$\langle n_L, 0, n_R | H | n_L, 0, n_R \rangle \ll \langle n_L, n_M, n_R | H | n_L, n_M, n_R \rangle, \quad (21)$$

for  $n_{L/R} \in \{0, 1\}$ , and  $n_M > 0$ . Thus, the states with zero occupation in the middle dot form our low-energy manifold.

Occupied states in the middle dot are separated by an energy  $\sim \Delta$  from the low-energy manifold. In the weak coupling limit  $t \ll \Delta$ , the high-energy subspace only contributes

to the low-energy dynamics through virtual processes. Therefore, we use a Schieffer-Wolff transformation to obtain the effective Hamiltonian in the low-energy subspace in Eq. (6). Whenever  $\mu_L = \mu_R = 0$ , the terms in Eq. (6) for the anti-parallel spin configuration are:

$$\epsilon_R^{\uparrow\downarrow} = \kappa (-2B \sin^2(\theta_R) + B + \mu_M), \quad \epsilon_L^{\uparrow\downarrow} = \kappa (-2B \cos^2(\theta_L) + B + \mu_M), \quad (22)$$

$$\Lambda_{\uparrow\downarrow} = \kappa \Delta \cos(\theta_L + \theta_R), \quad \Gamma_{\uparrow\downarrow} = -i\kappa [\mu_M \cos(\theta_L + \theta_R) - B \sin(\theta_L - \theta_R)], \quad (23)$$

and for the parallel configuration:

$$\epsilon_R^{\uparrow\uparrow} = \kappa (-2B \cos^2(\theta_R) + B + \mu_M), \quad \epsilon_L^{\uparrow\uparrow} = \kappa (-2B \cos^2(\theta_L) + B + \mu_M), \quad (24)$$

$$\Lambda_{\uparrow\uparrow} = -i\kappa \Delta \sin(\theta_L + \theta_R), \quad \Gamma_{\uparrow\uparrow} = -\kappa [\mu_M \cos(\theta_L + \theta_R) - B \cos(\theta_L - \theta_R)], \quad (25)$$

where

$$\kappa = t^2 / (\Delta^2 + \mu_M^2 - B^2). \quad (26)$$

At finite  $B$ , the chemical potential  $\mu_M$  at which  $\Gamma_{\sigma_i \sigma_j} = 0$  shifts to:

$$\mu_{\text{shift}}^{\uparrow\downarrow} = \frac{B \sin(\theta_L - \theta_R)}{\sin(\theta_L + \theta_R)}, \quad \mu_{\text{shift}}^{\uparrow\uparrow} = \frac{B \cos(\theta_L - \theta_R)}{\cos(\theta_L + \theta_R)}, \quad (27)$$

for anti-parallel and parallel spin configurations.

## B Convenience of the anti-parallel spin configuration

### B.1 Orthogonality with symmetric spin precession

In Eq. (22) for the anti-parallel spin configuration we notice that when the spin precession angles are equal  $\theta_L = \theta_R = \theta$ , the double occupation onsite energy  $\epsilon_L + \epsilon_R = 0$  is zero at  $\mu_M = 0$  and the ETC minima shifts disappear as shown in Eq. (27). That restores the orthogonality of operations within the even parity sector and thus we express  $\mathcal{U}_3(\gamma)$  operation as:

$$\mathcal{U}_3(\gamma) = \exp \left[ -\frac{i}{\hbar} H_P(\{\mu_{L/R}\}) \tau_P^{(2)} \right] \times \exp \left[ -\frac{i}{\hbar} H_P(\{t\}) \tau_P^{(1)} \right], \quad (28)$$

where we compensate a finite  $\epsilon_L - \epsilon_R$  with an onsite pulse. On the other hand, the hopping operation requires additional operations to compensate for non-orthogonality [35]:

$$\begin{aligned} \mathcal{U}_2(\beta) &= \exp \left[ -\frac{i}{\hbar} H_P(\{\mu_L = \mu, \mu_R = \mu\}) \tau_P^{(N+4)} \right] \times \exp \left[ -\frac{i}{\hbar} H_P(\{t\}) \tau_P^{(N+3)} \right] \\ &\times \exp \left[ -\frac{i}{\hbar} H_P(\{\mu_L = \mu, \mu_R = \mu\}) \tau_P^{(N+2)} \right] \times \exp \left[ -\frac{i}{\hbar} H_P(\{\mu_{L/R}\}) \tau_P^{(N+1)} \right] \\ &\times \prod_{j=1}^{N/2} \exp \left[ -\frac{i}{\hbar} H_P(\{t, \mu_M\}) \tau_P^{(2j)} \right] \times \exp \left[ -\frac{i}{\hbar} H_P(\{\mu_{L/R}\}) \tau_P^{(2j-1)} \right] \end{aligned} \quad (29)$$

where  $N$  is the number of pulses required to correct for the non-orthogonality within the odd parity sector.

## B.2 Stability and number of operations

To quantify the degree of linear dependence of the operations, we define the following metric

$$\mathcal{L}_o = \sqrt{\frac{(\epsilon_L - \epsilon_R)^2}{(\epsilon_L - \epsilon_R)^2 + \Gamma^2}}, \quad (30)$$

$$\mathcal{L}_e = \sqrt{\frac{(\epsilon_L + \epsilon_R)^2}{(\epsilon_L + \epsilon_R)^2 + \Lambda^2}} \quad (31)$$

for  $\mathcal{L}_e$  even  $\mathcal{L}_o$  and odd fermion parity sectors. If  $\mathcal{L}_{e/o} = 0$ , the operations are orthogonal and the scheme outlined in Section 4 is valid. On the other hand, if  $\mathcal{L}_{e/o} = 1$ , it is impossible to generate a universal set of operations. To understand how robust the scheme in Eq. (28) is, we consider small deviations from the perfect spin precession case:  $\theta_L = \theta$  and  $\theta_R = \theta + \delta$ . In this case, the metric  $\mathcal{L}_{e/o}$  reads:

$$\mathcal{L}_o = \left[ 1 + \left( \frac{\mu_M}{B} \tan 2\theta \right)^2 \right]^{-1/2} + O(\delta), \quad (32)$$

$$\mathcal{L}_e = \delta \left( \frac{B}{\Delta} \right) \tan 2\theta + O(\delta^2). \quad (33)$$

Depending on the linear dependence  $\mathcal{L}_{e/o}$  of the hopping and pairing operations, we can estimate the maximal number of pulses required to implement an arbitrary operation [35] within a given fermion parity subspace:

$$\mathcal{N}(\mathcal{L}_{e/o}) = \left\lceil \frac{\pi}{\arccos(\mathcal{L}_{e/o})} \right\rceil + 1. \quad (34)$$